

Interaction of Two Dielectric Macroparticles

V. R. Munirov^{a,b} and A. V. Filippov^{a,*}

^a Troitsk Institute for Innovation and Fusion Research, Moscow, Troitsk, 142190 Russia

*e-mail: fav@triniti.ru

^b Moscow Institute of Physics and Technology (State University), Dolgoprudnyi, Moscow oblast, 141700 Russia

Received May 15, 2013

Abstract—The electrostatic interaction of two charged dielectric spherical particles with a nonuniform free-charge distribution over their surfaces in an external homogeneous electric field is considered. An exact solution for the electric field potential is obtained, and an analytical expression for the interaction force between these two particles is found. The case of a uniform free-charge distribution is considered in detail, and the region of parameters in the plane “the ratio of the radii vs. the ratio of the charges,” where repulsion between two like-charged particles turns into attraction as the interparticle distance decreases is established.

DOI: 10.1134/S1063776113130050

1. INTRODUCTION

The problem of the interaction of two spherical particles has long history. In 1811, Poisson used expansion into Legendre polynomials to solve the problem of interaction of two spherical particles made of a conducting material (see [1, 2]). Then, Kelvin solved this problem employing the image method and expansion into Legendre polynomials in a bispherical coordinate system [3]. Maxwell found an interaction potential using expansion into Legendre polynomials in a spherical coordinate system accurate to R^{-22} terms, where R is the distance between particles' centers [4]. In that work, he obtained the expansion of Legendre polynomials with a pole located at the center of one particle into Legendre polynomials with a pole at the center of the other particle by differentiation method (for detail, see [5]). Russel [6] derived expressions for capacitance coefficients at small distances between the particle surfaces, $L = (R - a_1 - a_2)$. These expressions were also obtained in [7, 8] and used to answer the question of whether attraction exists between the particles at short distances.

The problem of interaction of two spherical particles can only be solved in the form of a sum of an infinite series, which rather slowly converges at small interparticle distances, even if they are made of a conducting material. Therefore, it is necessary to use numerical methods and solutions can only be obtained for particular cases. Many aspects of this interaction and the methods for obtaining solutions for the case of conducting balls are reflected in [7–26], while the effect of an external homogeneous electric field on the interaction of two uncharged and charged spherical particles made of a conducting material was studied in [27, 28].

Since the investigation of the interaction of dielectric particles is a more complex problem, the history of solving this problem is shorter and it was investigated in a smaller number of works [29–40]. The authors of [29, 30] analyzed the interaction of two identical uncharged dielectric particles in an external electric field. Love [29] obtained a solution for any angle between the external field direction and the axis of symmetry of the problem, which passes through the centers of the particles, while Goyette [30] found a solution only for the parallel and perpendicular directions. Stoy [31, 32] considered particles having different sizes and different permittivities in an electric field directed along the line connecting the centers of the particles [31] and perpendicular to it [32]. Ymeri [33] analyzed the case of identical particles at an arbitrary external field direction, and the case of different particles was studied in [34]. In [29–34], the problem was solved in a bispherical coordinate system.

Feng [35] numerically investigated the interaction of two charged dielectric particles in contact with each other using the Galerkin finite element method. In [36], the problem of two charged spherical particles was solved in a spherical coordinate system by the reexpansion of Legendre polynomials with a pole located at the center of one of the particles into Legendre polynomials with a pole at the center of the other particle.¹ The authors of [37] used this method to analyze the interaction of two uniformly charged dielectric spheres and determined the parameter region in which like-charged dielectric spheres attract

¹ In [36], this method of solution was called the Washizu method [41, 42]. As noted above, this method was used by Maxwell [4] and explicit expressions for the reexpansion of Legendre polynomials are given in [5].

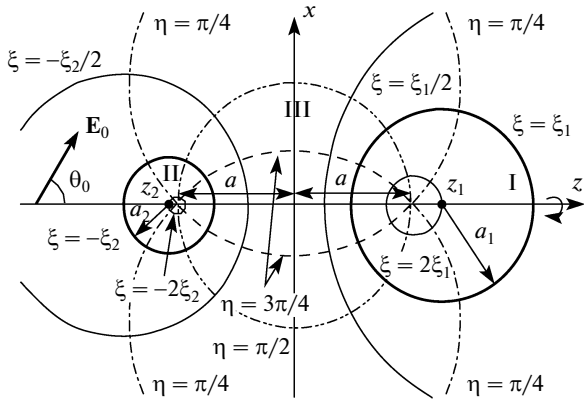


Fig. 1. Geometry of the interaction of two macroparticles of radii a_1 and a_2 in the bispherical coordinate system (ξ, η, φ) .

each other at short distances. Then, the authors of [38–40] used the analytical model created in [37] to study the interaction of carbon clusters and fullerenes [38, 39], and dielectric particles in a dielectric solvent [40].

Note that Filippov [18, 19] investigated the interaction of a point charge with a spherical conducting macroparticle in a plasma; in [43], we analyzed the interaction of a point charge with a dielectric macroparticle in a plasma with a homogeneous external electric field.

The purpose of this work is to solve the problem of the electrostatic interaction of two nonuniformly charged dielectric spherical particles of different radii placed in a homogeneous dielectric in a homogeneous external electric field.

2. CALCULATION OF POTENTIAL EXPANSION COEFFICIENTS

We consider two spherical particles with radii a_1 and a_2 , charges q_1 and q_2 (which are nonuniformly distributed over their surfaces in the general case), and dielectric constants ε_1 and ε_2 that are placed in a homogeneous dielectric (dielectric constant ε) and homogeneous (before the placement of the particles) electric field E_0 . A Cartesian coordinate system is introduced so that the electric-field vector lies in plane xz and axis z is directed along the line connecting the centers of the particles (see Fig. 1).

We then introduce bispherical coordinates as shown in Fig. 1 [44, 45],

$$x = \frac{a \sin \eta \cos \varphi}{\cosh \xi - \cos \eta}, \quad y = \frac{a \sin \eta \sin \varphi}{\cosh \xi - \cos \eta},$$

$$z = \frac{a \sinh \xi}{\cosh \xi - \cos \eta},$$

where

$$\cosh \xi_1 = \frac{R^2 + a_1^2 - a_2^2}{2Ra_1}, \quad \cosh \xi_2 = \frac{R^2 + a_2^2 - a_1^2}{2Ra_2},$$

$$R = z_1 - z_2 = a(\coth \xi_1 + \coth \xi_2)$$

$$= a_1 \cosh \xi_1 + a_2 \cosh \xi_2,$$

$$a = a_1 \sinh \xi_1 = a_2 \sinh \xi_2,$$

$$z_1 = a \coth \xi_1 = a_1 \cosh \xi_1,$$

$$z_2 = -a \coth \xi_2 = -a_2 \cosh \xi_2.$$

The electrostatic interaction of particles in a homogeneous dielectric is determined by the Laplace equation $\Delta \phi = 0$; in the bispherical coordinates, it can be solved by the separation of variables and the introduction of a new quantity

$$\phi(\xi, \eta, \varphi) = \psi(\xi, \eta, \varphi) \sqrt{\cosh \xi - \cos \eta},$$

where ϕ is the electrostatic field potential. The bounded solutions of the Laplace equation in the bispherical coordinates inside and outside the particles can be represented as follows:

$$\psi_I(\xi, \eta, \varphi)$$

$$= \sum_{l=0}^{\infty} \sum_{m=0}^l [A_l^m \cos(m\varphi) + A_l^{-m} \sin(m\varphi)] \quad (1)$$

$$\times e^{-(l+1/2)\xi} P_l^m(\cos \eta),$$

$$\psi_{II}(\xi, \eta, \varphi)$$

$$= \sum_{l=0}^{\infty} \sum_{m=0}^l [B_l^m \cos(m\varphi) + B_l^{-m} \sin(m\varphi)] \quad (2)$$

$$\times e^{(l+1/2)\xi} P_l^m(\cos \eta),$$

$$\psi_{III}(\xi, \eta, \varphi)$$

$$= \sum_{l=0}^{\infty} \sum_{m=0}^l \{ [C_l^m \cos(m\varphi) + C_l^{-m} \sin(m\varphi)] e^{-(l+1/2)\xi} \quad (3)$$

$$+ [D_l^m \cos(m\varphi) + D_l^{-m} \sin(m\varphi)] e^{(l+1/2)\xi} \} P_l^m(\cos \eta).$$

The potential of a homogeneous external electric field has the form

$$\phi_0 = -E_{0x} \frac{a \sin \eta \cos \varphi}{\cosh \xi - \cos \eta} - E_{0z} \frac{a \sinh \xi}{\cosh \xi - \cos \eta}, \quad (4)$$

where $E_{0x} = E_0 \sin \theta_0$ and $E_{0z} = E_0 \cos \theta_0$. Its expansion into Legendre polynomials in the introduced bispherical coordinate system is determined by the expression

$$\phi_0 = -\sqrt{2} a E_{0z} \operatorname{sgn} \xi \sqrt{\cosh \xi - \cos \eta}$$

$$\times \sum_{l=0}^{\infty} (2l+1) e^{-(l+1/2)|\xi|} P_l(\cos \eta) \quad (5)$$

$$- 2\sqrt{2} a E_{0x} \sqrt{\cosh \xi - \cos \eta}$$

$$\times \sum_{l=1}^{\infty} e^{-(l+1/2)|\xi_l|} P_l^1(\cos \eta) \cos \varphi.$$

The resulting potential in region III is the sum of Eqs. (3) and (5) due to the principle of superposition.

The following boundary conditions result from the continuity of the potential and the discontinuity of the normal components of the electric displacement field [46]:

$$\phi|_{\xi=\xi_1-0} = \phi|_{\xi=\xi_1+0}, \quad \phi|_{\xi=-\xi_2-0} = \phi|_{\xi=-\xi_2+0}, \quad (6)$$

$$\varepsilon \frac{1}{h_\xi} \frac{\partial \phi}{\partial \xi} \Big|_{\xi=\xi_1-0} - \varepsilon_1 \frac{1}{h_\xi} \frac{\partial \phi}{\partial \xi} \Big|_{\xi=\xi_1+0} = 4\pi\sigma_1, \quad (7)$$

$$\varepsilon_2 \frac{1}{h_\xi} \frac{\partial \phi}{\partial \xi} \Big|_{\xi=-\xi_2-0} - \varepsilon \frac{1}{h_\xi} \frac{\partial \phi}{\partial \xi} \Big|_{\xi=-\xi_2+0} = 4\pi\sigma_2,$$

where σ_1 and σ_2 are the surface densities of free charges on the first and second macroparticle, respectively, and h_ξ is the Lamé coefficient (see below). In the general case, the surface densities are functions of η and φ .

To find the distribution of free surface charges, it is better to use a spherical coordinate system with the origin placed at the center of each of the particles,

$$\sigma_i(\theta_i, \varphi) = \sum_{n=0}^{\infty} \sum_{m=0}^n (\sigma_{i,n}^m \cos m\varphi + \sigma_{i,n}^{-m} \sin m\varphi) \times P_n^m(\cos \theta_i), \quad i = 1, 2, \quad (8)$$

where θ_i is the latitude of a point on the surface of the i th particle in the spherical coordinate system with the pole at its center and φ is the longitude of this point. In the Appendix, we show that the expansion of distribution (8) into Legendre polynomials in the bispherical coordinate system has the form

$$\sigma_i(\theta_i, \varphi) = \sqrt{\cosh \xi_i - \cos \eta} \times \sum_{l=0}^{\infty} \sum_{m=0}^l (\tilde{\sigma}_{i,l}^m \cos m\varphi + \tilde{\sigma}_{i,l}^{-m} \sin m\varphi) \times e^{-(l+1/2)|\xi_l|} P_l^m(\cos \eta), \quad i = 1, 2; \quad (9)$$

where

$$\tilde{\sigma}_{i,l}^{\pm m} = \sum_{n=m}^{\infty} b_{i,l}^{nm} \sigma_{i,n}^{\pm m}, \quad (10)$$

$$b_{i,l}^{nm} = 2^{m+1/2} e^{-(n-m)\xi_i} \sinh^m \xi_i \frac{(l-m)!}{(l+m)!} \times \sum_{v=0}^{\min(l,n)-m} (-1)^{n-m+v} e^{2v\xi_i} \times \frac{(l+n-v)!}{v!(n-m-v)!(l-m-v)}. \quad (11)$$

From the continuity condition of potential (6), we express coefficients $A_l^{\pm m}$ and $B_l^{\pm m}$ in terms of $C_l^{\pm m}$ and

$D_l^{\pm m}$. Then, using condition (7) and the properties of associated Legendre functions [5] after simple but tedious algebra, we obtain the following equations for the potential expansion coefficients:

$$\mathbb{A}_l^{\pm m} \mathbf{y}_{l-1} + \mathbb{C}_l^{\pm m} \mathbf{y}_l + \mathbb{B}_l^{\pm m} \mathbf{y}_{l+1} = \mathbf{F}_l^{\pm m}; \quad (12)$$

$$l = 0, 1, \dots, \infty, \quad m = 0, 1, \dots, l,$$

where

$$\mathbf{y}_l = \begin{pmatrix} C_l^{\pm m} \\ D_l^{\pm m} \end{pmatrix},$$

$$\mathbb{A}_l^{\pm m} = (l-m)$$

$$\times \begin{pmatrix} (\varepsilon - \varepsilon_1) e^{-(l-1/2)\xi_1} & -(\varepsilon + \varepsilon_1) e^{(l-1/2)\xi_1} \\ -(\varepsilon + \varepsilon_2) e^{(l-1/2)\xi_2} & (\varepsilon - \varepsilon_2) e^{-(l-1/2)\xi_2} \end{pmatrix}, \quad (13)$$

$$(\mathbb{C}_l^{\pm m})_{11} = (\varepsilon - \varepsilon_1) [\sinh \xi_1 - (2l+1) \cosh \xi_1] \times e^{-(l+1/2)\xi_1},$$

$$(\mathbb{C}_l^{\pm m})_{12} = [(\varepsilon - \varepsilon_1) \sinh \xi_1 + (2l+1)(\varepsilon + \varepsilon_1) \cosh \xi_1] \times e^{(l+1/2)\xi_1}, \quad (14)$$

$$(\mathbb{C}_l^{\pm m})_{21} = [(\varepsilon - \varepsilon_2) \sinh \xi_2 + (2l+1)(\varepsilon + \varepsilon_2) \cosh \xi_2] \times e^{(l+1/2)\xi_2},$$

$$(\mathbb{C}_l^{\pm m})_{22} = (\varepsilon - \varepsilon_2) [\sinh \xi_2 - (2l+1) \cosh \xi_2] e^{-(l+1/2)\xi_2}, \quad \mathbb{B}_l^{\pm m} = (l+m+1)$$

$$\times \begin{pmatrix} (\varepsilon - \varepsilon_1) e^{-(l+3/2)\xi_1} & -(\varepsilon + \varepsilon_1) e^{(l+3/2)\xi_1} \\ -(\varepsilon + \varepsilon_2) e^{(l+3/2)\xi_2} & (\varepsilon - \varepsilon_2) e^{-(l+3/2)\xi_2} \end{pmatrix}, \quad (15)$$

$$\mathbf{F}_l^1 = 2a \{ 4\pi \tilde{\sigma}_{1,l} + (\varepsilon - \varepsilon_1) \sqrt{2} E_{0z} \}$$

$$\times [\cosh \xi_1 - (2l+1) \sinh \xi_1] e^{-(l+1/2)\xi_1}, \quad (16)$$

$$\mathbf{F}_l^2 = 2a \{ 4\pi \tilde{\sigma}_{2,l} - (\varepsilon - \varepsilon_2) \sqrt{2} E_{0z} \} \times [\cosh \xi_2 - (2l+1) \sinh \xi_2] e^{-(l+1/2)\xi_2},$$

$$\mathbf{F}_l^{1,2}$$

$$= \begin{pmatrix} 2a [4\pi \tilde{\sigma}_{1,l} - (\varepsilon - \varepsilon_1) 2\sqrt{2} E_{0x} \sinh \xi_1] e^{-(l+1/2)\xi_1} \\ 2a [4\pi \tilde{\sigma}_{2,l} - (\varepsilon - \varepsilon_2) 2\sqrt{2} E_{0x} \sinh \xi_2] e^{-(l+1/2)\xi_2} \end{pmatrix}, \quad (17)$$

$$\mathbf{F}_l^{\pm m} = \begin{pmatrix} 8\pi a \tilde{\sigma}_{1,l}^{\pm m} e^{-(l+1/2)\xi_1} \\ 8\pi a \tilde{\sigma}_{2,l}^{\pm m} e^{-(l+1/2)\xi_2} \end{pmatrix}. \quad (18)$$

This set of equations represents a system with a block three-diagonal matrix. A number of numerical

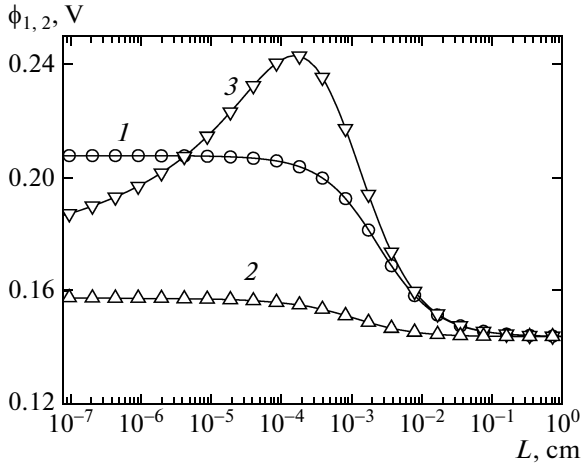


Fig. 2. Macroparticle surface potentials vs. the minimum distance between the particle surfaces at (1) $a_1 = a_2 = 10 \mu\text{m}$ and $q_1 = q_2 = 10^3 e$; (2), (3) $a_1 = 10 \mu\text{m}$, $a_2 = 1 \mu\text{m}$, $q_1 = 10^3 e$, and $q_2 = 10^2 e$ ((2) surface potential of the larger particle, (3) that of the smaller particle). (solid curves) Calculations performed in this work at $\varepsilon_1 = \varepsilon_2 = 10^5$ for $\eta = 0$, (symbols) calculations for macroparticles made of a conducting material at $\varepsilon_1 = \varepsilon_2 = \infty$ according to [18, 19].

methods were developed to solve such problems, and here we use the matrix sweep and the reduction methods [47]. (In [34], the solution to this set was obtained in the form of infinite continued fractions for the case of uncharged particles.)

Figure 2 shows the dependences of the macroparticle surface potential on the minimum distance between the particle surfaces ($L = (R - a_1 - a_2)$) for the case of a high dielectric constant ($\varepsilon_1 = \varepsilon_2 = 10^5$) for particles with the same and different radii. At such a high dielectric constant, the particles behave like metallic particles; therefore, the potential remains almost unchanged over the entire macroparticle surface. (The data for $\eta = 0$ and π , where the potential has extreme values, almost coincide. For example, at $L = 10^{-7}$ cm, the ratio of the near-surface potentials in the case of particles of the same size at $\eta = 0$ and π differs from unity by 8.4×10^{-6} .) These data agree well with the similar curve for metallic macroparticles from [18, 19]. We now calculate the interparticle interaction force.

3. CALCULATION OF THE INTERACTION FORCE

To calculate the resultant force applied to a dielectric body, we can use the Maxwell stress tensor [46] (calculations are performed for the first particle, which is located on the side of positive values of axis z ;

therefore, the repulsive force from the second particle is positive for it and the attractive force is negative),

$$\mathbf{F} = \oint_S \mathbf{T}_{1n} dS, \quad (19)$$

where

$$\begin{aligned} \mathbf{T}_{1n} &= \frac{\varepsilon}{4\pi} \left(E_n \mathbf{E} - \frac{1}{2} \mathbf{n} E^2 \right) \Big|_{\xi = \xi_1} \\ &\equiv \frac{\varepsilon}{4\pi} \left(\frac{1}{2} (E_n^2 - E_\tau^2) \mathbf{n} + E_n E_\tau \boldsymbol{\tau} \right) \Big|_{\xi = \xi_1}, \end{aligned} \quad (20)$$

$$E_n = \frac{1}{h_\xi} \frac{\partial \phi}{\partial \xi} \Big|_{\xi = \xi_1}, \quad \mathbf{n} = -\mathbf{e}_\xi;$$

$$E_\tau = -\frac{1}{h_\eta} \frac{\partial \phi}{\partial \eta} \Big|_{\xi = \xi_1}, \quad \boldsymbol{\tau} = \mathbf{e}_\eta;$$

and \mathbf{e} is the orthonormal basis vectors. Note that

$$(\mathbf{e}_\xi \cdot \mathbf{e}_z) = -\cos \theta, \quad (\mathbf{e}_\eta \cdot \mathbf{e}_z) = -\sin \theta.$$

For the force on the first particle, from Eqs. (19) and (20) we find (all quantities in the formulas are assumed to be taken at $\xi = \xi_1$)

$$\begin{aligned} F_{1x} &= \frac{\varepsilon}{4\pi} \int \left[\frac{1}{2} (E_\xi^2 - E_\eta^2 - E_\varphi^2) \frac{\sinh \xi \sin \eta \sin \varphi}{\cosh \xi - \cos \eta} \right. \\ &+ E_\xi E_\eta \frac{(1 - \cosh \xi \cos \eta) \cos \varphi}{\cosh \xi - \cos \eta} + E_\xi E_\varphi \sin \varphi \left. \right] \\ &\times h_\eta h_\varphi d\eta d\varphi, \end{aligned} \quad (21)$$

$$\begin{aligned} F_{1y} &= \frac{\varepsilon}{4\pi} \int \left[\frac{1}{2} (E_\xi^2 - E_\eta^2 - E_\varphi^2) \frac{\sinh \xi \sin \eta \sin \varphi}{\cosh \xi - \cos \eta} \right. \\ &+ E_\xi E_\eta \frac{(1 - \cosh \xi \cos \eta) \sin \varphi}{\cosh \xi - \cos \eta} - E_\xi E_\varphi \cos \varphi \left. \right] \\ &\times h_\eta h_\varphi d\eta d\varphi, \end{aligned} \quad (22)$$

$$\begin{aligned} F_{1z} &= \frac{\varepsilon}{4\pi} \int \left[\frac{1}{2} (E_\xi^2 - E_\eta^2 - E_\varphi^2) \frac{\cosh \xi \cos \eta - 1}{\cosh \xi - \cos \eta} \right. \\ &+ E_\xi E_\eta \frac{\sinh \xi \sin \eta}{\cosh \xi - \cos \eta} \left. \right] h_\eta h_\varphi d\eta d\varphi, \end{aligned} \quad (23)$$

where h_ξ , h_η , and h_φ are the Lamé coefficients. In the bispherical coordinate system they are expressed as [45]

$$h_\xi = h_\eta = \frac{a}{\cosh \xi - \cos \eta}, \quad h_\varphi = \frac{a \sin \eta}{\cosh \xi - \cos \eta}. \quad (24)$$

Using the properties of the associated Legendre polynomials [5, 44, 45, 48, 49], after tedious algebra we express the force of interaction of nonuniformly charged dielectric spheres in a homogeneous dielectric

in the presence of a homogeneous external electric field as

$$\begin{aligned}
 F_{1x} = & \frac{\varepsilon}{4} \sum_{l=1}^{\infty} l(l+1) [D_l^1 (\tilde{C}_{l-1} + \tilde{C}_{l+1} - 2\tilde{C}_l) \\
 & - \tilde{C}_l^1 (D_{l-1} + D_{l+1} - 2D_l)] \\
 & + \frac{\varepsilon}{8} \sum_{l=2m=1}^{\infty} \sum_{l-1}^{l-1} \frac{(l+m+1)!}{(l-m-1)!} \\
 & \times [D_l^{m+1} (\tilde{C}_{l-1}^m + \tilde{C}_{l+1}^m - 2\tilde{C}_l^m) \\
 & + D_l^{-(m+1)} (\tilde{C}_{l-1}^{-m} + \tilde{C}_{l+1}^{-m} - 2\tilde{C}_l^{-m}) \\
 & - \tilde{C}_l^{m+1} (D_{l-1}^m + D_{l+1}^m - 2D_l^m) \\
 & - \tilde{C}_l^{-(m+1)} (D_{l-1}^{-m} + D_{l+1}^{-m} - 2D_l^{-m})],
 \end{aligned} \quad (25)$$

$$\begin{aligned}
 F_{1y} = & \frac{\varepsilon}{4} \sum_{l=1}^{\infty} l(l+1) [D_l^{-1} (\tilde{C}_{l-1} + \tilde{C}_{l+1} - 2\tilde{C}_l) \\
 & - \tilde{C}_l^{-1} (D_{l-1} + D_{l+1} - 2D_l)] \\
 & + \frac{\varepsilon}{8} \sum_{l=2m=1}^{\infty} \sum_{l-1}^{l-1} \frac{(l+m+1)!}{(l-m-1)!} \\
 & \times [D_l^{-(m+1)} (\tilde{C}_{l-1}^m + \tilde{C}_{l+1}^m - 2\tilde{C}_l^m) \\
 & - D_l^{m+1} (\tilde{C}_{l-1}^{-m} + \tilde{C}_{l+1}^{-m} - 2\tilde{C}_l^{-m}) \\
 & - \tilde{C}_l^{-(m+1)} (D_{l-1}^m + D_{l+1}^m - 2D_l^m) \\
 & + \tilde{C}_l^{m+1} (D_{l-1}^{-m} + D_{l+1}^{-m} - 2D_l^{-m})],
 \end{aligned} \quad (26)$$

$$\begin{aligned}
 F_{1z} = & \frac{\varepsilon}{4} \sum_{l=0m=0}^{\infty} \sum_{l-1}^l (2l+1) \frac{(l+m)!}{(l-m)!} \\
 & \times (\tilde{C}_l^m D_l^m + \tilde{C}_l^{-m} D_l^{-m}) \\
 & - \frac{\varepsilon}{4} \sum_{l=0m=0}^{\infty} \sum_{l-1}^l \frac{(l+m+1)!}{(l-m)!} [(\tilde{C}_l^m D_{l+1}^m + \tilde{C}_l^{-m} D_{l+1}^{-m}) \\
 & + (\tilde{C}_{l+1}^m D_l^m + \tilde{C}_{l+1}^{-m} D_l^{-m})].
 \end{aligned} \quad (27)$$

Here, $\tilde{C}_l = C_l - (2l+1)\sqrt{2}aE_{0z}$, $\tilde{C}_l^1 = C_l^1 - 2\sqrt{2}aE_{0x}$, $\tilde{C}_l^{-1} = C_l^{-1}$, $\tilde{C}_l^{\pm m} = C_l^{\pm m}$, and $m > 1$, and we assume that $C_l^{-m} = C_l^m$ and $D_l^{-m} = D_l^m$ at $m = 0$.

In the case of uniformly charged particles in the absence of an external electric field, it follows from

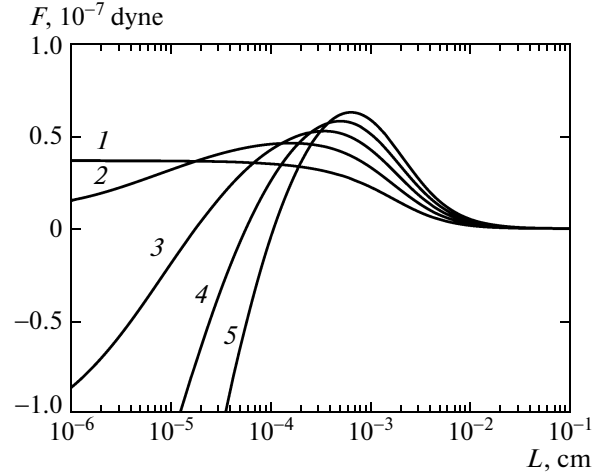


Fig. 3. Interaction force between uniformly charged dielectric spheres in vacuum ($\varepsilon = 1$) vs. the minimum distance between their surfaces $L = R - a_1 - a_2$ for various ratios of their charges at $a_1 = a_2 = 10^{-3}$ cm, $q_1 = 10^3 e$, and $\varepsilon_1 = \varepsilon_2 = 25$: $q_1/q_2 = (1) 1.0$ (2) 1.5, (3) 2.0, (4) 2.5, and (5) 3.

Eqs. (25)–(27) that only the z component of the force is nonzero,

$$\begin{aligned}
 F_{1z} = & \frac{\varepsilon}{2} \sum_{n=0}^{\infty} C_n \\
 & \times [(2n+1)D_n - (n+1)D_{n+1} - nD_{n-1}] \\
 & \equiv \frac{\varepsilon}{2} \sum_{n=0}^{\infty} D_n [(2n+1)C_n - (n+1)C_{n+1} - nC_{n-1}].
 \end{aligned} \quad (28)$$

4. ATTRACTION OF LIKE AND UNIFORMLY CHARGED PARTICLES

The repulsion between like-charged particles can turn into their attraction at short distances because of mutually induced charges on their surfaces. For example, it is known that, in the case of interaction of a point charge with a like-charged conducting or dielectric sphere, they begin to attract each other at short distances [45]. Further, we will study the interaction of two dielectric spherical particles having the same sign charges uniformly distributed over their surfaces. For definiteness, we assume $\varepsilon = 1$.

Figure 3 shows the dependence of the interaction force of the same-size particles with $\varepsilon_1 = \varepsilon_2 = 25$ on the minimum distance between the macroparticle surfaces for various ratios of the charges. Negative forces correspond to attraction and positive forces to repulsion. It is seen that, as the ratio of charges increases, the repulsion of like-charged macroparticles changes into attraction. For the dielectric constant under study, this change occurs at $q_1/q_2 = 1.5$ –2 (more specifically at $q_1/q_2 \approx 1.556$; as the ratio of charges decreases, this change takes place at $q_1/q_2 \approx 0.6426$,

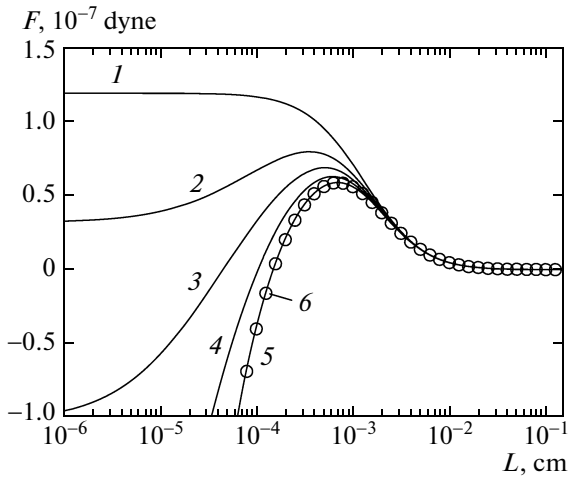


Fig. 4. Interaction force between uniformly charged dielectric spheres in vacuum vs. the minimum distance between their surfaces for various dielectric constants at $a_1 = a_2 = 10 \mu\text{m}$, $q_2 = 10^3 e$, and $q_1 = 3q_2$: $\epsilon_1 = \epsilon_2 = (1)$ 2 (2) 5, (3) 10, (4) 25, and (5) 10^3 . (6) Calculations for metallic particles ($\epsilon_1 = \epsilon_2 = \infty$) according to [18, 19].

which is the reciprocal of the previous number (see below)).

Figure 4 shows how the interaction of two spheres of the same radius and a charge ratio $q_1/q_2 = 3$ changes with their dielectric constant. It is clear that an increase in the dielectric constant leads to a decrease in the repulsive force at long distances and to the change of repulsion into attraction at short distances

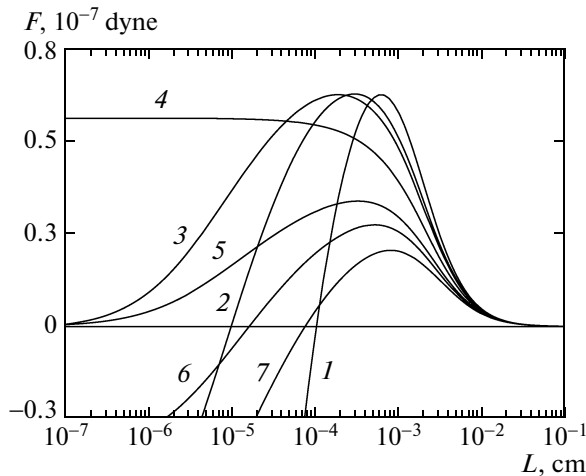


Fig. 5. Interaction force between spherical particles in vacuum ($\epsilon = 1$) vs. the minimum distance between their surfaces for various ratios of their radii a_1/a_2 at $a_2 = 10 \mu\text{m}$, $q_1 = 3q_2$, $q_2 = 10^3 e$, $\epsilon_1 = \epsilon_2 = 25$: $a_1/a_2 = (1)$ 1 (2) 1.3, (3) 1.425, (4) 1.828, (5) 2.345, (6) 2.6, and (7) 3.0.

(this change takes place at a dielectric constant between 5 and 10), and the attractive force increases with the dielectric constant. It is also seen that, at a high dielectric constant, the force almost coincides with the force of metallic particles.

Figure 5 shows the interaction force of dielectric particles with $\epsilon_1 = \epsilon_2 = 25$ and charges $q_1 = 3q_2$ for various ratios of their radii. It is seen that the effect of attraction disappears and again appears as the ratio of radii a_1/a_2 increases. This behavior becomes clear from Fig. 6, which shows (for several dielectric constants of the particles) the curves bounding the parameter region in the $(a_1/a_2, q_1/q_2)$ plane where the attraction of like-charged dielectric particles does not manifest itself (this region lies between the curves having indices 1 and 2 at the same letter for each dielectric constant). Curve 3 in Fig. 5 corresponds to the point of intersection of curve C_2 with the straight line $q_1/q_2 = 3$ in Fig. 6, and curve 5 corresponds to the point of intersection of this straight line with curve C_1 .

We now show that the boundaries of the region where attraction effects are absent are only determined by the ratios of the radii and the charges of uniformly charged particles. To this end, we write equations to calculate the potential expansion coefficients for the case of a uniform distribution of a free charge over the particle surfaces in a medium without an external electric field. Then, dividing the obtained equations by $2\sqrt{2} \epsilon \sqrt{q_1 q_2 / a_1 a_2}$ and using Eqs. (12)–(16), for the case under study we find

$$(1 - \kappa_1) l e^{\xi_1} \tilde{C}_{l-1} - (1 + \kappa_1) l e^{2\xi_1} \tilde{D}_{l-1}$$

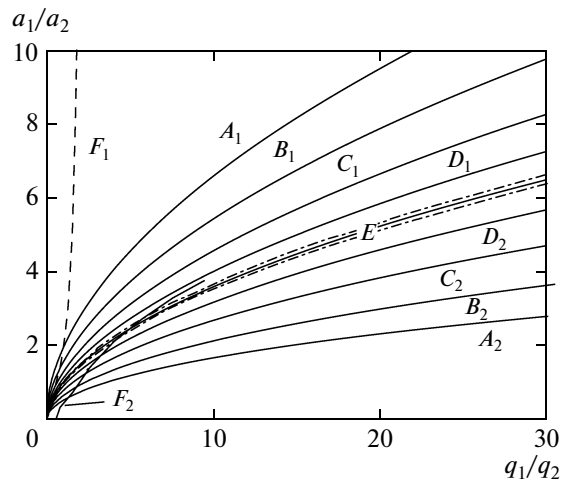


Fig. 6. Curves separating the regions of attraction and repulsion of like and uniformly charged macroparticles in the $(a_1/a_2, q_1/q_2)$ plane for various values of their dielectric constants. Attraction is absent at any distances in the region between curves A_1 and A_2 , B_1 and B_2 , and so on. $\kappa_1 = \kappa_2 = (A_1, A_2)$ 5, (B_1, B_2) 10, (C_1, C_2) 25, (D_1, D_2) 81, and (dot-and-dash lines) 1000. Curve E corresponds to Eq. (35) for conducting macroparticles. (F_1, F_2) Digitized data for $\kappa_1 = \kappa_2 = 25$ from [37].

$$\begin{aligned}
 & + (1 - \kappa_1)[\sinh \xi_1 - (2l + 1)\cosh \xi_1]\tilde{C}_l \\
 & + [(1 - \kappa_1)\sinh \xi_1 + (2l + 1)(1 + \kappa_1)\cosh \xi_1] \\
 & \quad \times e^{(2l+1)\xi_1}\tilde{D}_l \tag{29} \\
 & + (l + 1)(1 - \kappa_1)e^{-\xi_1}\tilde{C}_{l+1} - (l + 1) \\
 & \quad \times (1 + \kappa_1)e^{2(l+1)\xi_1}\tilde{D}_{l+1} \\
 & = \sqrt{\frac{q_1 a_2}{q_2 a_1}} \sinh \xi_1,
 \end{aligned}$$

$$\begin{aligned}
 & -(1 + \kappa_2)le^{2l\xi_2}\tilde{C}_{l-1} + (1 - \kappa_2)le^{\xi_2}\tilde{D}_{l-1} \\
 & + [(1 - \kappa_2)\sinh \xi_2 + (2l + 1)(1 + \kappa_2)\cosh \xi_2]e^{(2l+1)\xi_2}\tilde{C}_l \\
 & + (1 - \kappa_2)[\sinh \xi_2 - (2l + 1)\cosh \xi_2]\tilde{D}_l \tag{30} \\
 & - (l + 1)(1 + \kappa_2)e^{2(l+1)\xi_2}\tilde{C}_{l+1} + (l + 1)(1 - \kappa_2) \\
 & \quad \times e^{-\xi_2}\tilde{D}_{l+1} = \sqrt{\frac{q_2 a_1}{q_1 a_2}} \sinh \xi_2,
 \end{aligned}$$

where new coefficients and relative dielectric constants are introduced,

$$\begin{aligned}
 \tilde{C}_l &= \frac{C_l}{2\sqrt{2}}\sqrt{\frac{a_1 a_2}{q_1 q_2}}, \quad \tilde{D}_l = \frac{D_l}{2\sqrt{2}}\sqrt{\frac{a_1 a_2}{q_1 q_2}}, \tag{31} \\
 \kappa_1 &= \frac{\epsilon_1}{\epsilon}, \quad \kappa_2 = \frac{\epsilon_2}{\epsilon}.
 \end{aligned}$$

Allowing for the fact that

$$\xi_1 = \xi_1\left(\frac{a_1}{a_2}, \frac{L^2}{a_1 a_2}\right), \quad \xi_2 = \xi_2\left(\frac{a_1}{a_2}, \frac{L^2}{a_1 a_2}\right),$$

from Eqs. (29) and (30) we obtain

$$\begin{aligned}
 \tilde{C}_l &= \tilde{C}_l\left(\frac{q_1}{q_2}, \frac{a_1}{a_2}, \frac{L^2}{a_1 a_2}, \kappa_1, \kappa_2\right), \tag{32} \\
 \tilde{D}_l &= \tilde{D}_l\left(\frac{q_1}{q_2}, \frac{a_1}{a_2}, \frac{L^2}{a_1 a_2}, \kappa_1, \kappa_2\right).
 \end{aligned}$$

When substituting Eqs. (31) and (32) into Eq. (28), we find

$$F_{1z} = \epsilon \frac{q_1 q_2}{a_1 a_2} f\left(\frac{q_1}{q_2}, \frac{a_1}{a_2}, \frac{L^2}{a_1 a_2}, \kappa_1, \kappa_2\right), \tag{33}$$

where f is the unknown function of the arguments. As follows from Eq. (33), the presence or absence of attraction at short distances depends only on relative quantities q_1/q_2 , a_1/a_2 , κ_1 , and κ_2 rather than on their absolute values (of course, the force depends on them). Since the exact boundary is determined by the equation $F_{1z} = 0$ at $L = 0$, its position is a function of only q_1/q_2 , a_1/a_2 , κ_1 , and κ_2 .

It is seen in Fig. 6 that, as the dielectric constant increases, the region where attraction is absent narrows gradually and transforms into a curve with a zero

area for conducting particles ($\epsilon_{1,2} \rightarrow \infty$). This problem for conducting particles was studied in detail in [8] using asymptotic expressions for capacitance coefficients at $L \rightarrow 0$ [6, 7],

$$\begin{aligned}
 C_{11} &= \frac{a_1 a_2}{a_1 + a_2} \\
 & \times \left[\frac{1}{2} \ln \frac{2a_1 a_2}{(a_1 + a_2)L} - \psi\left(\frac{a_2}{a_1 + a_2}\right) + O(L) \right], \\
 C_{22} &= \frac{a_1 a_2}{a_1 + a_2} \tag{34} \\
 & \times \left[\frac{1}{2} \ln \frac{2a_1 a_2}{(a_1 + a_2)L} - \psi\left(\frac{a_1}{a_1 + a_2}\right) + O(L) \right], \\
 C_{12} &= -\frac{a_1 a_2}{a_1 + a_2} \left[\frac{1}{2} \ln \frac{2a_1 a_2}{(a_1 + a_2)L} + \gamma + O(L) \right],
 \end{aligned}$$

where $\psi(z) = d \ln \Gamma(z) / dz$ is the logarithmic derivative of the gamma function (or digamma function) and γ is the Euler constant ($\gamma = 0.5772156649\dots$).

Lekner [8] showed that attraction does not manifest itself if spherical conductors have charges at the ratio that would be observed if they were in electrical contact with each other, when the potentials of their surfaces become exactly equal to each other. Using the capacitance coefficients given above, we can find the electric field energy, differentiate it, and see that the interaction force becomes repulsive only under the condition [8]

$$\frac{q_1}{q_2} = \frac{\gamma + \psi\left(\frac{a_2}{a_1 + a_2}\right)}{\gamma + \psi\left(\frac{a_1}{a_1 + a_2}\right)}. \tag{35}$$

Grashchenkov [21] concluded that attraction always manifests itself when the ratio of the charges of conducting spheres differs from the ratio of their charges after they are brought into electrical contact. He found the condition of equality of the surface potentials,

$$\frac{q_1}{q_2} = \frac{C_{11} + C_{12}}{C_{12} + C_{22}}, \tag{36}$$

which exactly transforms into Eq. (35) after the substitution of Eqs. (34).

It is seen in Fig. 6 that the regions where attraction manifests itself at short distances and the region where like-charged particles undergo only repulsion are separated by two curves. We now introduce quantity $y = a_1/a_2$ and designate these curves as $y_1(x)$ and $y_2(x)$, where $x = q_1/q_2$. The position of a zero point should not change at $\kappa_1 = \kappa_2$ during the permutation of the particles because of the equality of the forces on the first and second particles. Therefore, the relations

$$y_1(x) = y_2^{-1}(x^{-1}), \quad y_2(x) = y_1^{-1}(x^{-1})$$

should occur between these functions. Indeed, at certain $q_1/q_2 = x$, the boundary between the regions lies at

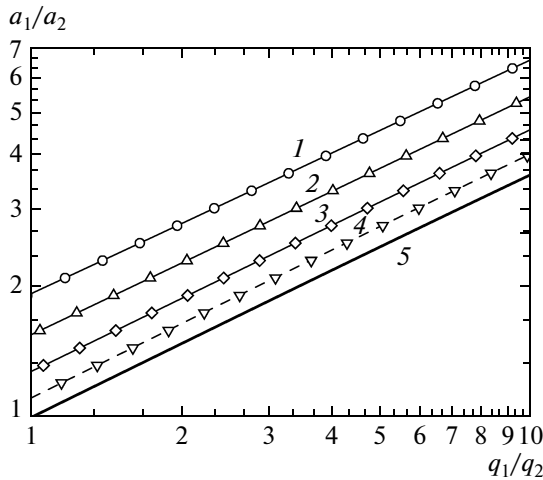


Fig. 7. Boundaries of the regions of attraction and repulsion of like and uniformly charged macroparticles on the logarithmic scale. (1)–(4) $y_1(x)$ curves and (symbols) $y_2^{-1}(x^{-1})$ curves. (1) and symbols (\circ) for $\epsilon_1 = \epsilon_2 = 5$, (2) and (\triangle) 10, (3) and (\diamond) 25, (4) and (∇) 81, and (5) curve according to Eq. (35) for conducting macroparticles.

points $a_1/a_2 = y_1(x)$ and $a_1/a_2 = y_2(x)$; upon the permutation of the particles at $q_2/q_1 = x^{-1}$, it lies at points $a_2/a_1 = y_1^{-1}(x)$ and $a_2/a_1 = y_2^{-1}(x)$. Figure 7 shows the $y_1(x)$ and $y_2^{-1}(x^{-1})$ curves that are coincident (in the case of conductors, this coincidence is clearly visible from Eq. (35)). It is also visible that the behavior of the curves is similar and they are close to straight lines when the ratio of particle charges changes at various dielectric constants (this is true of only the range of the ratio of the radii under study). Therefore, they can be presented in the form

$$y_1(x) = kx^\alpha, \quad y_2(x) = k^{-1}x^\alpha,$$

and the power $\alpha \approx 0.56$ remains almost the same for different dielectric constants of the particles, while coefficient k increases with decreasing ϵ_1 and ϵ_2 .

Figure 8 shows the product of functions $x_1(y)$ and $x_2(y^{-1})$, which are the reciprocal functions of $y_1(x)$ and $y_2(x)$. This product is seen to be close to unity; however, as the ratio of the radii increases or decreases, the difference from unity increases and becomes slightly larger than 0.1% at $a_1/a_2 = 0.1$ and 10 for $\epsilon_1 = \epsilon_2 = 81$. Note that the data in Figs. 6–8 were calculated with the maximum number of terms taken into account to calculate the force ($l_{\max} = 2^{16}$) at the minimum distance between the particle surfaces $L = 10^{-9}$ cm. The values of ratio q_1/q_2 at which the force becomes zero at a given ratio of the radii was determined at $a_2 = 10 \mu\text{m}$ and $q_2 = 10^3 e$, where e is the elementary charge. The difference of the product of functions $x_1(y)$ and $x_2(y^{-1})$ from unity is related to the fact that the roots of the

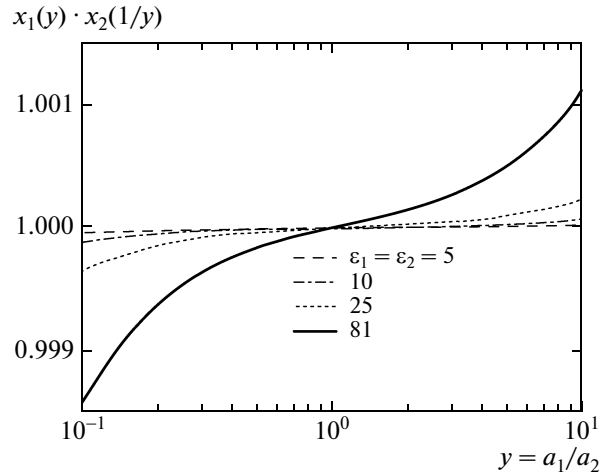


Fig. 8. Product of the $x_1(y)$ and $x_2(y^{-1})$ functions that determine the boundaries of the regions of attraction and repulsion of like and uniformly charged macroparticles in the $(y = a_1/a_2, x = q_1/q_2)$ plane for various values of their dielectric constants.

equation $F_{1z} = 0$ were found at a finite distance ($L = 10^{-9}$ cm) rather than for contact between the particles. The force is still positive for an “exact” ratio of the charges at the boundary of the regions at this distance. For a constant interparticle distance, the reduced distances $\tilde{L} = L/\sqrt{a_1 a_2}$ for $a_1/a_2 = 0.1$ and $a_1/a_2 = 10$ differ by an order of magnitude. If the boundary is calculated at $\tilde{L} = 10^{-6}$, the maximum difference (in absolute value) of the product $x_1(y)x_2(y^{-1})$ from unity in the range $0.1 \leq y \leq 10$ is 3.8×10^{-8} (also see Table 1).

This high accuracy of determining the product $x_1(y)x_2(y^{-1})$ does not allow us to judge about the accuracy of determining the boundary position and only indicates that the position of the point where the force becomes zero is only determined by the ratios of the radii and charges. For example, Filippov [18] showed that, at $a_1 = a_2$ and $q_1/q_2 = 1.0035$, attraction between conducting spheres appears at a distance $L \leq 10^{-10}$ cm (see Fig. 12 in [18]), although repulsion is absent at all distances only for the exact equality $q_1 = q_2$.

The data in Table 1 can be used to estimate the accuracy of determining the position of the boundary. As the reduced distance decreases, the relative accuracy of determining the ratio of charges at the boundary increases and becomes better than 0.05% at $\tilde{L} = 10^{-6}$. (Note that Table 1 gives the ratios of charges at the boundaries only to the seventh digit and that quantities f_1, f_2 , and f_3 were calculated from the initial ratios of the charges, which were accurate to the fifteenth decimal digit.)

The authors of [37] also determined the boundaries of attraction and repulsion regions. However, these

Table 1. Ratio of the charges at the upper and lower boundaries of the regions with attraction at short distances and without attraction at any distances for various values of the reduced distance between the surfaces of dielectric particles with $\kappa_1 = \kappa_2 = 81$, $l_{\max} = 2^{17}$ terms taken into account, and $a_2 = 10^{-3}$ cm

$L/\sqrt{a_1 a_2}$		10^{-7}	10^{-6}	10^{-5}	10^{-4}	10^{-3}
$a_1 = 0.1a_2$	x_1	0.011231	0.011226	0.011177	0.010824	0.009398
$(y = 0.1)$	x_2	54.51514	54.49613	54.31719	53.04312	48.03530
$a_1 = 0.1a_2$	x_1	0.830659	0.830513	0.829102	0.817913	0.765078
$(y = 1)$	x_2	1.203864	1.204076	1.206124	1.222623	1.307056
$a_1 = 10a_2$	x_1	0.018344	0.018350	0.018410	0.018853	0.020818
$(y = 10)$	x_2	89.04120	89.08239	89.47332	92.38390	106.40605
	f_1^a	1.899	6.429	-2.572	3.284	-0.661
	f_2^b	4.881	-5.095	-2.521	2.701	-1.702
	f_3^c	0.250	1.847	-3.416	-2.692	-0.946

Note: $^a f_1 = [x_1(y=1)x_2(y=1) - 1] \times 10^{11}$, $^b f_2 = [x_1(0.1)x_2(10) - 1] \times 10^9$, $^c f_3 = [x_1(10)x_2(0.1) - 1] \times 10^9$.

results differ noticeably from our data (see Fig. 6) and are not symmetric with respect to the permutation of the particles.² It is seen that curves F_1 and F_2 differ rather strongly from curves C_1 and C_2 , and that F_2 even intersects the curve for conducting particles. It should also be noted that there is a q_2/q_1 region (up to 2 at $\kappa_1 = \kappa_2 = 2$) in which no attraction between the particles occurs at $a_2 = 0$ (see Fig. 6 in [37]). Meanwhile, it is well known [45, 48] that attraction between point and dielectric particles of a spherical shape is absent only if $\epsilon_1 \leq \epsilon$, i.e., at $\kappa_1 \leq 1$, and that attraction at short distances inevitably takes place at $\kappa_1 > 1$. Then, at $\kappa_1 = \kappa_2 = 1000$, the interaction force of dielectric particles differs insignificantly from the case of conducting particles, and the curves separating attraction and repulsion regions should be close to curve E , which takes place in Fig. 6 in this work. In [37], the repulsion region for this dielectric constant is much wider.

The problem in [37] was solved in the spherical coordinate system, which led to an ordinary set of equations for determining the coefficients of multipole expansion of the potential. Table 2 gives the reduced forces (determined as $\tilde{F}_{1z} = F_{1z}a_1a_2/q_1q_2$) for two identical dielectric particles with $\kappa_1 = \kappa_2 = 2$ and $\kappa_1 = \kappa_2 = 1000$. In this work, the calculations are performed at $l_{\max} = 2^{16}$ (as the number of terms increases to $l_{\max} = 2^{17}$, the reduced force changes only by unity

² Although the boundaries of attraction and repulsion regions in [37] were constructed in plane ($a_2/a_1, q_2/q_1$), this fact is insignificant in the light of the considerations given above for the symmetry of the boundaries relative to the permutation of the particles.

in the last digit of the numbers given in Table 2). A comparison of the data given in Table 2 demonstrates that the accuracy of determining the reduced force in [37] was rather high, at least for particles of the same size, and the causes of the inaccurate determination of the boundaries of attraction and repulsion regions in [37] remain unclear. Note that we have

$$\tilde{F}_{1z} = F_{1z} \frac{a_1 a_2}{q_1 q_2} = \frac{4 \ln 2 - 1}{24 \ln^2 2} = 0.153725465$$

for conducting spheres of the same size and charge [3, 8] and that the calculations at $\epsilon_1 = \epsilon_2 = 10^5$ yield $\tilde{F}_{1z} = 0.153728821$ at $L = 10^{-10}$ cm, which allows us to judge about the accuracy of the calculations performed in this work. The calculations executed using the expressions presented in [18, 19] for conducting particles ($\epsilon_1 = \epsilon_2 = \infty$) yield $\tilde{F}_{1z} = 0.153725458$ at the same number of expansion terms and the same interparticle distance, which allows us to estimate the difference between the forces at $L = 0$ and $L = 10^{-10}$ cm.

Table 2. Reduced force of interaction ($F_{1z}a_1a_2/q_1q_2$) of two identical spherical particles at $L = 10^{-10}$ cm with $l_{\max} = 2^{16}$ terms taken into account in the calculation in this work and at $L = 0$ and $n = 30$ terms of the multipole expansion of the potential in [37]

	This work	[37]
$\kappa_1 = \kappa_2 = 2$	0.210013282363	0.2100132974
$\kappa_1 = \kappa_2 = 1000$	0.153866817435	0.153866795

CONCLUSIONS

We solved the problem of the interaction of two spherical dielectric particles in a homogeneous dielectric using bispherical coordinates. We derived an analytical expression for the potential and the force of interaction of two spherical particles in the most general case of a nonuniform free-charge distribution over their surfaces in the presence of a homogeneous external electric field. The interaction of particles of different sizes and different charges was studied in detail at several dielectric constants of the particle material for a uniform free-charge distribution. As a result, the parameter region in which the repulsion of like-charged particles changes into their attraction at short interparticle distances was determined.

APPENDIX

Derivation of the Expansion of a Surface Charge in the Bispherical Coordinate System

To obtain Eq. (9), we use the approach proposed in [50]. Since the product $R_i^n P_n^m(\cos\theta_i)$ is a harmonic function, it can be represented in the bispherical coordinate system as

$$\left(\frac{R_i}{a_i}\right) P_n^m(\cos\theta_i) = \sqrt{\cosh\xi - \cos\eta} \times \sum_{l \geq 0} b_{i,l}^{nm} e^{-(l+1/2)|\xi|} P_l^m(\cos\eta), \quad i = 1, 2, \quad (37)$$

where R_i is the radius vector from the center of the i th particle to the point of observation and θ_i is the angle between this radius vector and the positive direction of axis z .

To find expansion coefficients $b_{i,l}^{nm}$, we consider the limit $\eta \rightarrow 0$. In this limit, for $0 < |\xi| < \xi_i$ we have

$$\frac{R_i}{a_i} = (-e^{-\xi_i}) \frac{1 - e^{2\xi_i} e^{-|\xi|}}{1 - e^{-|\xi|}}, \quad \frac{\sin\theta_i}{\sin\eta} = \frac{a_i}{R_i} \frac{\sinh\xi_i}{\cosh\xi - 1}.$$

Allowing for the limit

$$\lim_{\eta \rightarrow 0} P_n^m(\cos\eta) = \sin^m \eta P_n^{(m)}(1)$$

we can rewrite Eq. (37) as

$$\left(\frac{R_i}{a_i}\right)^n \left(\frac{a_i}{R_i} \frac{\sinh\xi_i}{\cosh\xi - 1}\right)^m P_n^{(m)}(1) = \sqrt{\cosh\xi - 1} e^{-1/2|\xi|} \sum_{l \geq 0} b_{i,l}^{nm} e^{-l|\xi|} P_l^{(m)}(1). \quad (38)$$

Here, $P_n^{(m)}(1)$ is the m th derivative of Legendre polynomials for the argument equal to unity,

$$P_n^{(m)}(1) = \frac{(n+m)!}{2^m m! (n-m)!}. \quad (39)$$

Finally, we derive Eq. (11) by expanding the expression in the left-hand side of Eq. (38) in powers of $e^{-|\xi|}$.

ACKNOWLEDGMENTS

This work was supported in part by the Russian Foundation for Basic Research (project no. 12-02-01177a) and a grant of the President of the Russian Federation (project no. NSh-2447.2012.2).

REFERENCES

1. J. R. Hoffman, *André-Marie Ampère: Poisson's 1812 Electricity Memoir* (Cambridge University Press, Cambridge, 1995), p. 113.
2. R. W. Home, *Br. J. Hist. Sci.* **16**, 239 (1983).
3. W. Thomson, *Reprint of Papers on Electrostatics and Magnetism* (Macmillan, London, United Kingdom, 1884), p. 86.
4. J. C. Maxwell, *A Treatise on Electricity and Magnetism*, 3rd ed. (Clarendon, Oxford, United Kingdom, 1891; Nauka, Moscow, 1989).
5. E. W. Hobson, *The Theory of Spherical and Ellipsoidal Harmonics* (Cambridge University Press, Cambridge, 1931; Inostrannaya Literatura, Moscow, 1952).
6. A. Russell, *Proc. R. Soc. London, Ser. A* **82**, 524 (1909).
7. J. Lekner, *J. Electrostat.* **69**, 11 (2011).
8. J. Lekner, *Proc. R. Soc. London, Ser. A* **468**, 2829 (2012).
9. G. B. Jeffery, *Proc. R. Soc. London, Ser. A* **87**, 109 (1912).
10. A. Moussiaux and A. Ronveaux, *J. Phys. A: Math. Gen.* **12**, 423 (1979).
11. A. V. Khachatourian and A. O. Wistrom, *J. Phys. A: Math. Gen.* **33**, 307 (2000).
12. A. V. Khachatourian and A. O. Wistrom, *J. Colloid Interface Sci.* **242**, 52 (2001).
13. A. O. Wistrom and A. V. Khachatourian, *Aerosol Sci. Technol.* **35**, 865 (2001).
14. V. A. Saranin, *Phys.—Usp.* **42** (4), 385 (1999).
15. V. A. Saranin, *Phys.—Usp.* **45** (12), 1287 (2002).
16. E. A. Shcherba, A. I. Grigor'ev, and V. A. Koromyslov, *Tech. Phys.* **47** (1), 13 (2002).
17. Y. H. Su, *Phys. Fluids* **18**, 042108 (2006).
18. A. V. Filippov, *JETP* **109** (3), 516 (2009).
19. A. V. Filippov, *Contrib. Plasma Phys.* **49**, 433 (2009).
20. V. A. Saranin and V. V. Mayer, *Phys.—Usp.* **53** (10), 1067 (2010).
21. S. I. Grashchenkov, *Tech. Phys.* **56** (7), 914 (2011).
22. J. Lekner, *J. Electrostat.* **68**, 299 (2010).
23. J. Lekner, *J. Electrostat.* **69**, 559 (2011).
24. J. Lekner, *J. Electrostat.* **69**, 435 (2011).
25. J. Lekner, *J. Appl. Phys.* **111**, 076102 (2012).
26. K. Kolikov, D. Ivanov, G. Krastev, Y. Epitropov, and S. Bozhkov, *J. Electrostat.* **70**, 91 (2012).
27. M. H. Davis, *Q. J. Mech. Appl. Math.* **17**, 499 (1964).

28. D. J. O'Meara and D. A. Saville, *Q. J. Mech. Appl. Math.* **34**, 9 (1981).
29. J. D. Love, *Q. J. Mech. Appl. Math.* **28**, 449 (1975).
30. A. Goyette and A. Navon, *Phys. Rev. B: Solid State* **13**, 4320 (1976).
31. R. D. Stoy, *J. Appl. Phys.* **65**, 2611 (1989).
32. R. D. Stoy, *J. Appl. Phys.* **66**, 5093 (1989).
33. H. M. Ymeri, *Electr. Eng. (Melbourne)* **80**, 227 (1997).
34. P. Chaumet and J. Dufour, *J. Electrostat.* **43**, 145 (1998).
35. J. Q. Feng, *Phys. Rev. E: Stat., Nonlinear, Soft Matter Phys.* **62**, 2891 (2000).
36. Y. Nakajima and T. Sato, *J. Electrostat.* **45**, 213 (1999).
37. E. Bichoutskaia, A. L. Boatwright, A. Khachatourian, and A. J. Stace, *J. Chem. Phys.* **133**, 024105 (2010).
38. A. J. Stace, A. L. Boatwright, A. Khachatourian, and E. Bichoutskaia, *J. Colloid Interface Sci.* **354**, 417 (2011).
39. A. J. Stace and E. Bichoutskaia, *Phys. Chem. Chem. Phys.* **13**, 18339 (2011).
40. A. J. Stace and E. Bichoutskaia, *Soft Matter* **8**, 6210 (2012).
41. M. Washizu, *J. Electrostat.* **29**, 177 (1993).
42. M. Washizu and T. B. Jones, *J. Electrostat.* **33**, 187 (1994).
43. V. R. Munirov and A. V. Filippov, *JETP* **115** (3), 527 (2012).
44. P. M. Morse and H. Feshbach, *Methods of Theoretical Physics* (McGraw Hill, New York, 1953).
45. V. V. Batygin and I. N. Toptygin, *Problems in Electrodynamics* (Nauka, Moscow, 1970; Academic, New York, 1978).
46. L. D. Landau and E. M. Lifshitz, *Course of Theoretical Physics, Volume 8: Electrodynamics of Continuous Media* (Butterworth-Heinemann, Oxford, 2004; Nauka, Moscow, 2005).
47. A. A. Samarskii and E. S. Nikolaev, *Numerical Methods for Grid Equations: Direct Methods* (Nauka, Moscow, 1978; Birkhauser, Boston, Massachusetts, United States, 1991).
48. W. R. Smythe, *Static and Dynamic Electricity*, 2nd ed. (Taylor and Francis, New York, 1950; Inostrannaya Literatura, Moscow, 1954).
49. T. M. MacRobert, *Spherical Harmonics*, 2nd ed., revised (Metiuen, London, United Kingdom, 1947).
50. M. S. Ingber and A. Zinchenko, *Int. J. Multiphase Flow* **42**, 152 (2012).

Translated by K. Shakhlevich